Grid Adaption for Problems in Fluid Dynamics

H. A. Dwyer*
University of California, Davis, California

This paper is concerned with the analysis and application of an adaptive grid technique to highly nonlinear problems in fluid mechanics and heat transfer. The analysis of the method shows that the percentage change in a dependent variable can be determined a priori, and that many problems with cell Reynolds number can be potentially overcome with grid adaption. In the application section of the paper, problems of external flow with separation, flame propagation, and shock/boundary-layer interaction have been solved to illustrate these properties. It is also shown that highly variable grid sizes caused by grid adaption do not cause accuracy problems when the solution and grid are coupled.

Introduction

OVER the past few years, a grid adaptive method developed by Dwyer et al.[1-3] has been used for a wide variety of problems involving heat transfer and flame propagation. Although the method has worked well, there has been very little analysis carried out on its mathematical properties, and it has not been applied to problems with very complex fluid dynamics. The purpose of the present paper is to perform some analysis of the method's properties and to solve some complex problems involving fluid dynamics. The results of both of these efforts have been very successful and it is now much clearer how and when grid adaption should be applied in complex problems. Also, the method has been extended to include grid adaption based on the influence of second derivatives, adding considerable usefulness to the technique. The paper will begin with the analysis of the method and then present physical problems which illustrate the attractive features of the technique as well as difficulties.

Method of Approach and Analysis

The basic method of adaption used does not involve the solution of an elliptic problem and does not significantly change the computational efforts involved for most problems. However, the method is dependent on the generation of an initial grid with certain properties. This point will be brought out clearly when two-dimensional problems will be solved. The purpose of this section is to define the properties of the technique and also illustrate some of these properties with one-dimensional examples.

The technique begins by adaption along arcs in space, and for the purpose of this introductory discussion the arcs will be assumed to already exist. The mathematical statement of the adaption technique is

$$\xi(x,y,t)=\int_0^s \left(1+b_1\left|\frac{\partial f}{\partial s}\right|+b_2\left|g\left(\frac{\partial^2 f}{\partial s^2}\right)\right|\right)\partial s \div \int_0^{s_{\max}} \left(1+b_1\left|\frac{\partial f}{\partial s}\right|+b_2\left|g\left(\frac{\partial^2 f}{\partial s^2}\right)\right|\right)\partial s$$

where ξ is one of the generalized coordinates associated with the transformation

$$x,y,t \rightarrow \xi,\eta,\tau$$

where s is the arc length, $s_{\max}$ the maximum arc length distance, f the dependent variable used for adaption, g some function of the second derivative of f to be chosen, and b_1 and b_2 weighting functions which determine the relative importance of adaption criteria. A useful interpretation of the above expression is that grid points will be distributed along a given arc length in space depending on the relative importance of the following factors: 1) total arc length and geometry, 2) dependent variable function variation, and 3) dependent variable slope variation.

In order to discuss these specific factors, it is useful to consider certain limits and ratios of the three terms. For example, if b_1 and b_2 are zero, it easily can be seen that the integral expression given above will yield a uniform and constant step-size distribution along the arc length s. A more interesting special case is $b_2=0$ and b_1 determined by the following equation:

$$b_1\int_0^{s_{\max}}\left|\frac{\partial f}{\partial s}\right|\partial s=\int_0^{s_{\max}}\partial s$$

or

$$b_1=\int_0^{s_{\max}}\partial s\Big/\int_0^{s_{\max}}\left|\frac{\partial f}{\partial s}\right|\partial s$$

This equality implies that arc length and function variation are weighted equally in the assignment of grid points. This relationship also can be used to insure a maximum limit on the variation of the function f between grid points. The integral of $|\partial f/\partial s|$ is the total variation of f over the arc length and if this total variation is assigned to have a value of 100%, then a quantitative statement of percentage change in Δf can be made. For example, if 100 grid points are to be distributed over the total arc length distance $s_{\max}$, then the above equality forces 50 of those points to be assigned solely due to Δf variation. Also, it follows directly that the maximum percentage change in f is less than 2% in this case. In general, the number of grid points assigned to function variation will be dependent upon the ratio R_1

$$R_1=b_1\int_0^{s_{\max}}\left|\frac{\partial f}{\partial s}\right|\partial s\Big/\int_0^{s_{\max}}\left(1+b_1\left|\frac{\partial f}{\partial s}\right|\right)\partial s$$

and the total number of grid points used. However, the maximum percentage change in f can always be determined a priori for any numerical simulation.

Presented as Paper 83-0449 at the AIAA 21st Aerospace Sciences Meeting, Reno, Nev., Jan. 10-13, 1983; submitted April 12, 1983; revision received Feb. 23, 1984.

*Professor of Mechanical Engineering; also Consultant, Sandia Laboratories, Livermore, Calif.

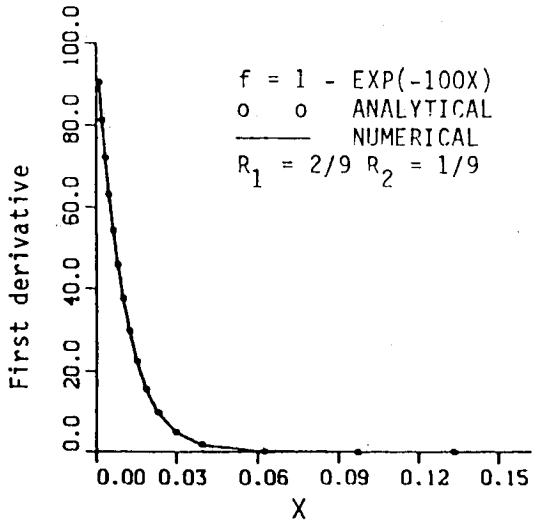

Fig. 1 Accuracy of derivative calculation with adaptive grid.

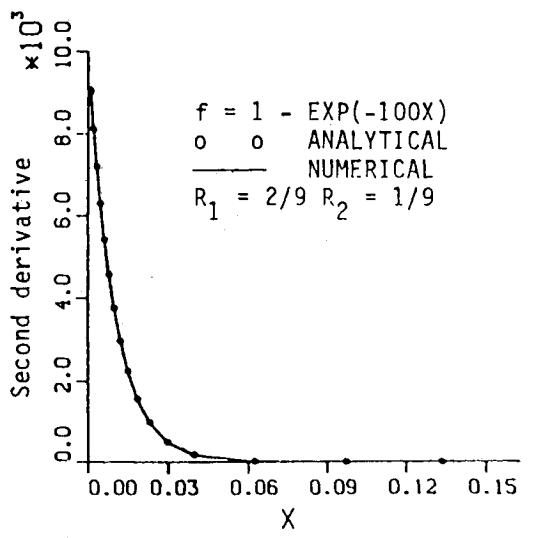

Fig. 2 Accuracy of derivative calculation with adaptive grid.

For the general case with second derivative adaption one can define two ratios which are important:

$$R_1 = b_1 \int_0^{s_{\max}} \left| \frac{\partial f}{\partial s} \right| \partial s \Big/ \int_0^{s_{\max}} \left(1 + b_1 \left| \frac{\partial f}{\partial s} \right| + b_2 \left| g\left(\frac{\partial^2 f}{\partial s^2} \right) \right| \right) \partial s$$

$$R_2 = b_2 \int_0^{s_{\max}} \left| g\left(\frac{\partial^2 f}{\partial s^2} \right) \right| \partial s \Big/ \int_0^{s_{\max}} \left(1 + b_1 \left| \frac{\partial f}{\partial s} \right| + b_2 \left| g\left(\frac{\partial^2 f}{\partial s^2} \right) \right| \right) \partial s$$

The first ratio, R_1, has exactly the same interpretation as previously given and it directly gives the percentage of grid points assigned to function variation. The second ratio, R_2, cannot be discussed completely until g is chosen, but the number of grid points assigned to second derivative dependence can be determined a priori, exactly as in the first derivative case.

In the present research three measures of second derivative dependence are used. It is best to place these measures in finite difference form since f is normally only known numerically. The three measures of second derivative used are

$$g_1 = \left| \frac{\dfrac{\Delta f^+}{\Delta s^+} - \dfrac{\Delta f^-}{\Delta s^-}}{\Delta s} \right|$$

$$g_2 = |\Delta f^+ - \Delta f^-|$$

$$g_3 = \left| \frac{\Delta f^+}{\Delta s^+} - \frac{\Delta f^-}{\Delta s^-} \right|$$

where

$$\Delta f^+ = f_{i+1} - f_i, \qquad \Delta f^- = f_i - f_{i-1}$$

$$\Delta s^+ = s_{i+1} - s_i, \qquad \Delta s^- = s_i - s_{i-1}$$

$$\Delta s = (\Delta s^+ + \Delta s^-)/2$$

All three of these measures have advantages and disadvantages and there does not seem to be any clear choice. However, when second derivative adaption is being employed, it is necessary to evaluate b_2 every adaptive step in order to keep the ratio R_2 fixed. This is particularly important since the second derivative is very grid sensitive and its integral could have very large variations in a given problem or from one grid to another.

The first function chosen, g_1, is the second derivative itself, and its integral can be dominated by a region of small radius of curvature. In fact, the major disadvantage of the second derivative is its complete dominance by a local region, however, depending on a physical problem it could be an advantage. The second function, g_2, is the second difference of f and is the least sensitive to sharp changes in slope. The third function, g_3, is a compromise between g_1 and g_2 and physically represents the change in slope between grid points. It can physically be seen that the reason for large local dependence is caused by dividing by a small Δs; however, in some problems this may be an attractive property. In general, we have used g_3 for most of our adaptive work, but the final choice should come from the physical problem and the convergence characteristics of the technique. Also, if the adaption technique is responsible for a solution-grid oscillation, then the g_2 choice or no second derivative adaption may be appropriate.

Numerical Experiments on Variable Step Size

The purpose of this section is to address, through numerical experiments, the question of inaccuracies caused by a rapid variation of grid size along a coordinate direction. It is generally well known, that a rapidly varying step size can be responsible for poor accuracy when using finite difference expressions. However, very little research has been done on studying the accuracy of finite difference expressions when used with adaptive techniques where the variable grid and function variation are strongly coupled. It is the purpose of this section to show that variable grids coupled with adaptive techniques are accurate, and that the previous problems encountered on nonadaptive grids do not seem to occur. It was hoped that mathematical analysis could be developed to prove this observation, but the present investigators have not succeeded in this pursuit. Therefore, a series of numerical experiments have been carried out on test problems to illustrate this feature of the method.

The test problems have been chosen to contain thin embedded regions with high gradients which may also have an interesting function variation inside the thin region. The two functions chosen are:

$$f_1 = 1 - e^{-\alpha x}, \qquad f_2 = 1 - e^{-\alpha x^2}$$

which were evaluated and applied over the region $0 \le x \le 1$. The numerical procedure consisted of starting from a uniform

grid and then applying the adaptive methods discussed above. As each new grid distribution was calculated, the function was again evaluated and the procedure was repeated until convergence was obtained. For all of the problems to be presented, convergence was obtained in less than eight iterations, and there was no problem of grid-solution oscillations with the technique.

The first problem solved consisted of the exponential function f_1 with $\alpha = 100$ and 40 grid points. The ratios R_1 and R_2 were chosen to be (the second derivative dependence g_3 was employed)

$$R_1 = 2/9, \qquad R_2 = 1/9$$

and these ratios guarantee that the maximum change in Δf between node points was less than 11.25%. The results of the grid adaption, along with the calculation of the first and second derivatives by the use of second-order central differences, are shown in Figs. 1 and 2. The dots in these graphs represent the grid locations as well as the exact analytical values of the first (Fig. 1) and second (Fig. 2) derivatives, while the solid lines without dots represent the numerically calculated derivatives. The expressions used to calculate the derivatives numerically were

$$f'_N = \frac{f_{i+1} - f_{i-1}}{s_{i+1} - s_{i-1}}$$

$$f''_N = \left[\left(\frac{f_{i+1} - f_i}{s_{i+1} - s_i}\right) - \left(\frac{f_i - f_{i-1}}{s_i + s_{i-1}}\right)\right] \Big/ \left(\frac{s_{i+1} - s_{i-1}}{2}\right)$$

which are simple and quite standard.

If a uniform grid was used for this problem, the first grid location would have been at $x = 0.025$, where the function takes on the value $f = 0.9179$. Any attempt to use the above formulas to calculate derivates numerically on this uniform grid will result in very inaccurate values. Also, a study of the figures clearly shows that the adaptive grid calculation gives very good accuracy, and no difference can be discerned between the numerical and exact calculations from the graphs. An objection that can be made to the results is that the forms of both the first and second derivatives are identical, and one would have much more difficulty with more complicated functions. Therefore, an investigation with the function f_2 was carried out.

Shown in Figs. 3 and 4 is an adaptive calculation with the same number of grid points and the same values of R_1 and R_2 for the function

$$f_2 = 1 - e^{-\alpha x^2}$$

with $\alpha = 1000$. Although the results are not bad, there is a noticeable error near $x = 0$ and in the region where the function approaches one. It easily can be recognized that this error is the result of the dramatically different forms of the first and second derivatives and the demands placed on the adaptive technique. The solution is to increase the value of R_1 and R_2 so that more grids are utilized in the high gradient regions. (This presents problems in resolving geometry in multidimensional problems, as will be discussed later in the paper.) Through numerical experimentation, good results were obtained for the following values of R_1 and R_2:

$$R_1 = 0.25, \qquad R_2 = 0.5$$

which imply that 75% of the points are being utilized in the high gradient regions. A noticeable feature of Figs. 5 and 6 is that the agreement is good even though the ratio of adjacent grid sizes approaches 3 at some locations. Conventional thinking would lead one to believe that very bad results would be achieved; however, the present results are not conventional because of the adaptive gridding employed.

Another important question which should be addressed is when adaption should not be employed. In general, it can be said that adaption is not of great usefulness when the gradients in f are "not steep." An example of "not steep" is for the function

$$f_2 = 1 - e^{-\alpha x^2}$$

with $\alpha = 10$. It can be quickly verified that a uniform grid will calculate the first and second derivatives accurately and there is little or no need for adaption. In general, the tradeoffs and usefulness of adaption will depend on the individual problem under consideration, but it definitely can be stated that adaption is needed for some problems. The paper will now direct itself to more complex problems in multidimensions.

Grid Adaption and Cell Reynolds Number

One of the key problems of computational fluid dynamics is the cell Reynolds number problem discussed in detail by Roach.[4] This flow problem results when a high gradient region occurs and the physical step size is larger or approximately the same size as the high gradient region. The reader should be reminded that this is only a problem with simultaneous convention and diffusion, and the problem vanishes in purely diffusive cases. For problems in fluid mechanics and heat transfer this implies that the Reynolds

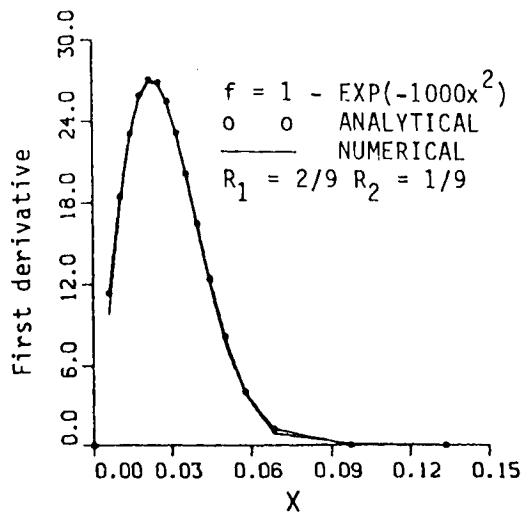

Fig. 3 Accuracy of derivative calculation with adaptive grid.

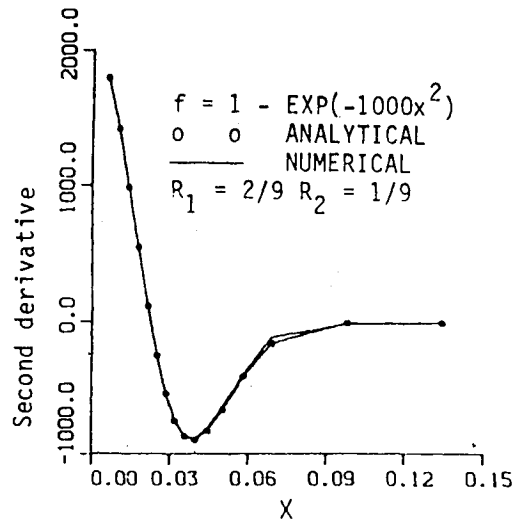

Fig. 4 Accuracy of derivative calculation with adaptive grid.

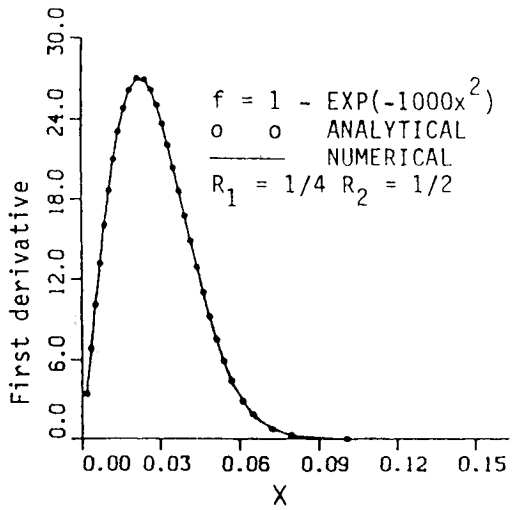

Fig. 5 Accuracy of derivative calculation with adaptive grid.

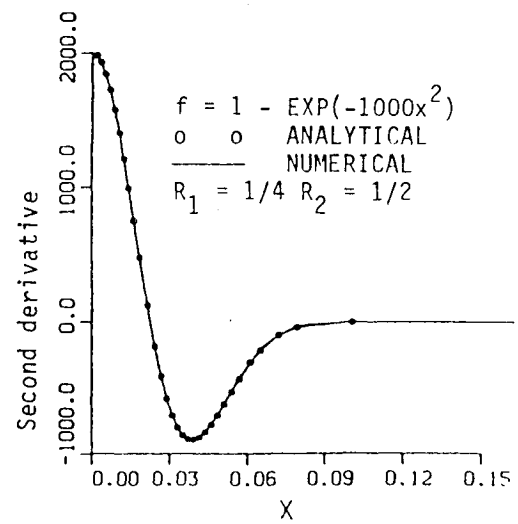

Fig. 6 Accuracy of derivative calculation with adaptive grid.

and Peclet numbers are large and, in general, throughout most of the flow region the characteristic time scale for convection is much shorter than diffusion.

For most numerical methods, the lack of resolution of high gradient convective-diffusive regions causes serious oscillations (second- and higher-order methods) or numerical diffusion (windward and first-order methods), and the overall calculation becomes inaccurate. It will be shown in the present paper that this problem usually can be removed with adaptive gridding and all numerical methods will work well. Before showing numerical examples, a short analysis will be performed to show what will be required of an adaptive technique if it is to resolve a thin convective-diffusive zone accurately.

Two examples of convective-diffusive regions are boundary layers and laminar flames; these regions typically have changes in the dependent variable of order one across them. Also, there is a characteristic velocity U which brings new fluid particles into the diffusive zone, along with a characteristic diffusion coefficient α. (For boundary layers it is important to remember that the characteristic velocity is the normal velocity at the edge and not the parallel flow velocity.) The characteristic time for convection across the zone is

$$\Delta t_v \simeq \delta/U$$

while that for diffusion is

$$\Delta t_D \simeq \delta^2/\alpha$$

where δ is the thickness of the convective-diffusive zone. Since the same fluid particles are involved in both convection and diffusion, these two time scales are approximately equal, and one obtains

$$\Delta t_v \simeq \delta/U \simeq \delta^2/\alpha \simeq \Delta t_D$$

or

$$U\delta/\alpha \simeq 0(1)$$

Thus, it is seen that on the scale of the high gradient zone the Reynolds or Peclet number is always one.

Also, it follows that Δf, the dependent variable change, is of order one across this region and the first derivative adaptive method can be adjusted easily to make the change in f less than 20%. Therefore, the grid Reynolds number $U\Delta x/\alpha$ will be considerably less than one in the high gradient region, and, hence, the problem is no longer a problem. First-order windward differences no longer generate serious artificial diffusion and, in fact, most numerical methods will yield good results.

In order to illustrate the above analysis, a flame propagation problem will be solved both with and without adaptive gridding. For this initial problem, the velocity field will be specified as Stokes flow over a spherical particle and the energy and species equations will be solved. The energy and species equations have the form

$$\frac{\partial}{\partial t}(\rho Z_m) + \frac{\partial}{\partial x}(\rho u Z_m) + \frac{\partial}{\partial y}(\rho v Z_m)$$
$$= \frac{\partial}{\partial x}\left(D_m \frac{\partial z_m}{\partial x}\right) + \frac{\partial}{\partial y}\left(D \frac{\partial Z_m}{\partial y}\right) + \dot{\omega}_m$$

where Z is the dependent variable vector (temperature and species mass fractions) and ω_m is the vector representing the chemical source terms:

$$Z = (T, Y_1, Y_2, \ldots, Y_K)^t$$

$$\dot{\omega} = (\dot{\omega}_T, \dot{\omega}_1, \dot{\omega}_2, \ldots, \dot{\omega}_K)^t$$

where ρ is the mass density, u the velocity in the x direction, v the velocity in the y direction, and D_m the diffusive transport coefficient for the mth equation. For the results presented in this paper, the equations were transformed to generalized cylindrical coordinates.[2]

The results of the calculations are shown in Figs. 7-12 and the following ratios of the time scales have been used:

$$\frac{\Delta t_D}{\Delta t_V} = 200 \text{ (Peclet number)}, \qquad \frac{\Delta t_D}{\Delta t \dot{\omega}_A} = 2.2 \times 10^5$$

where

$$\Delta t_D = U_\infty D/\alpha, \quad \Delta t_V = D/U_\infty$$

$$\Delta t_{\dot{\omega}A} = \text{chemical reaction time scale}$$

where D represents the spherical particle diameter and U_∞ the freestream velocity. With the time scales for convection and chemical reaction being much shorter than diffusion, a rather thin flame will develop around the spherical particle after an unsteady ignition period. This ignition period was started by raising the surface temperature of the particle and the chemistry and initial conditions were the same as the one-dimensional problems calculated previously.[3]

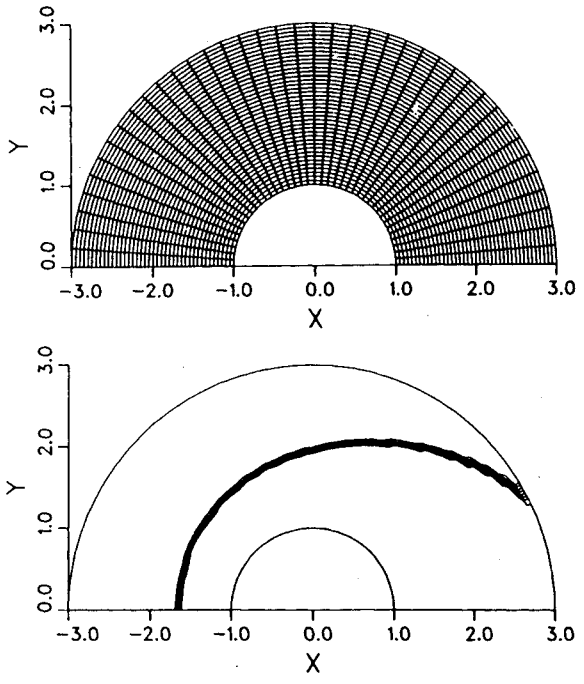

Fig. 7 Coordinate and isotherm distribution, uniform grid at early time.

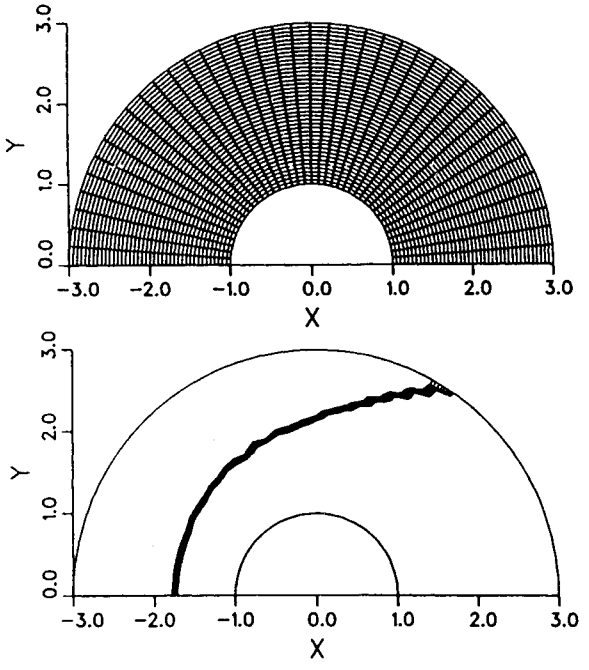

Fig. 8 Coordinate and isotherm distribution, uniform grid near termination.

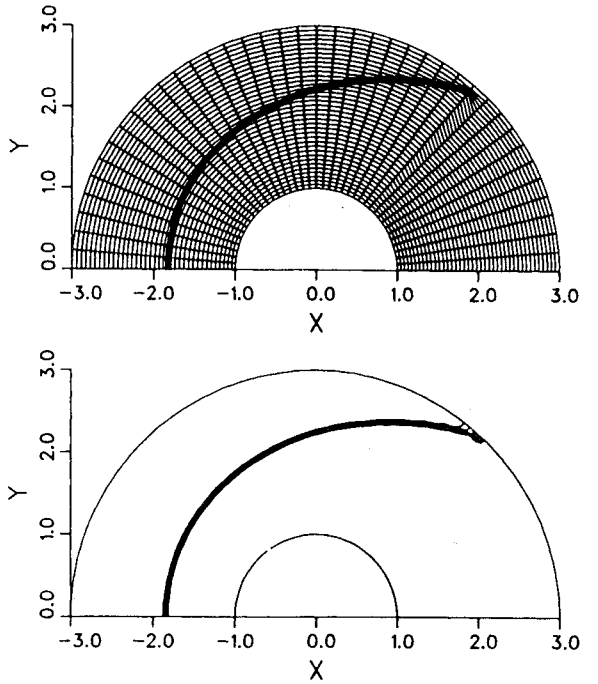

Fig. 9 Coordinate and isotherm distribution, adaptive grid at early time.

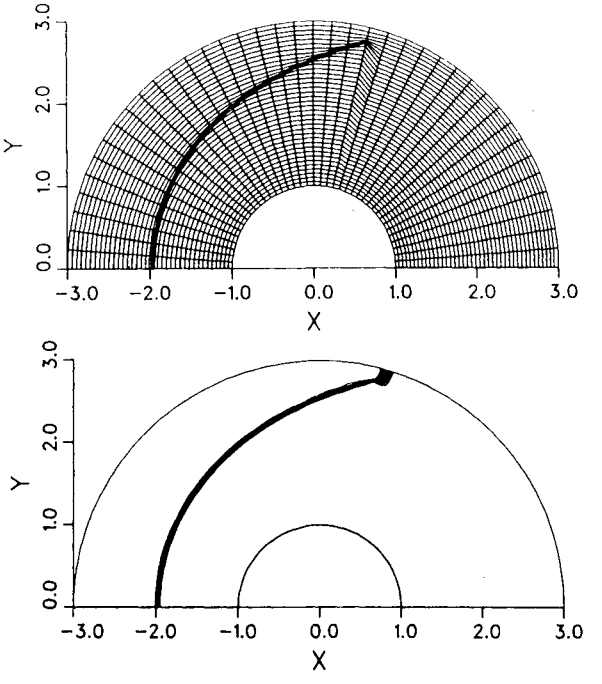

Fig. 10 Coordinate and isotherm distribution, adaptive grid at late time.

Figures 7 and 8 illustrate unsteady flame propagation after surface ignition when a uniform grid is employed. These figures are divided into two parts: the top shows the coordinate system, the bottom plots the isotherms, and there are 10 normalized isotherms plotted which range in value between 0.2 and 1.2. Originally, ignition occurred on the surface and the flame then propagates into and is convected by the flow. As the flame propagates away from the surface, the physical grid increases in size in the angular direction and the flame becomes parallel to the radial lines. Since central second-order finite differences have been used, the solution begins to oscillate because of the steep convective-diffusive zone compared to the grid size. Figure 8 represents the last time sequence in the calculation before the temperature becomes negative and thus the calculation terminates. If one changed the numerical calculation to windward differences the oscillations would disappear, but the flame speed would be inaccurate because of artificial diffusion influences. Therefore, another example of a typical cell Reynolds number problem is attained.

Now consider the problem using an adaptive grid as shown in Figs. 9 and 10. These figures show the coordinate and isotherm distributions for the same times as shown in Figs. 7 and 8. Notice that the flame has a new and more accurate velocity and position and there are no oscillations. By

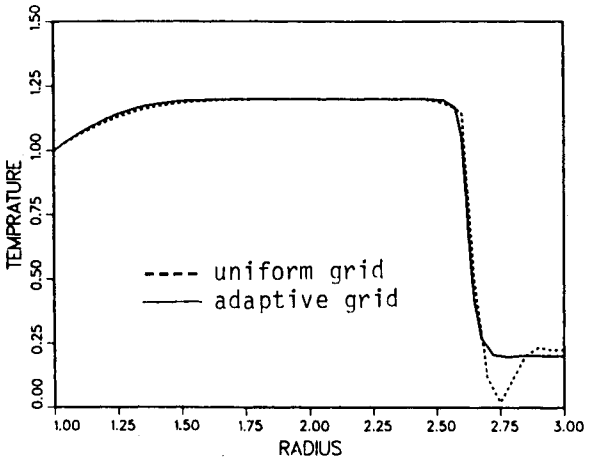

Fig. 11 Temperature distribution along a radial line with oscillations; --- uniform grid, —— adaptive grid.

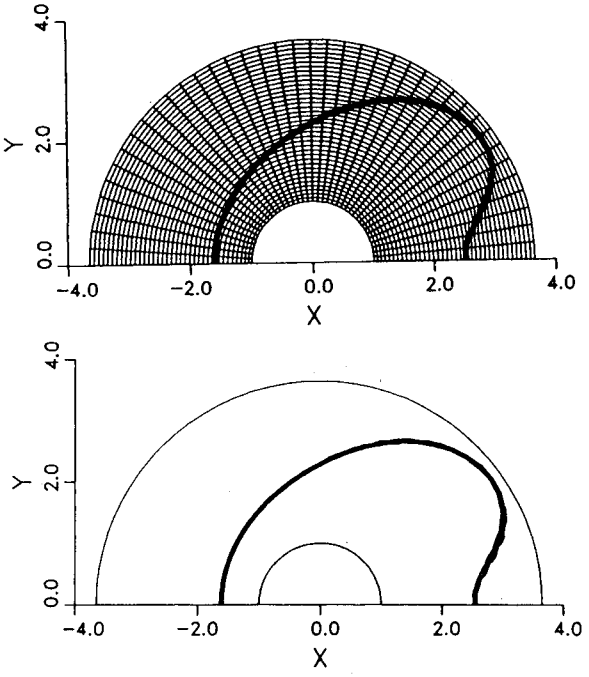

Fig. 12 Coordinate and isotherm distribution for separated flow with $Re = 100$.

resolving the flame, the cell Peclet number is reduced to values less than one. This guarantees that the solution will be oscillation-free. To illustrate the point further, the radial temperature distributions at similar angular positions are shown in Fig. 11 for both the uniform and adaptive grid solution. The oscillations in the uniform grid solution are quite apparent. The value of R_1 for the calculations was 1/7, which insured at least five points in the flame zone. Also, it should be mentioned that the uniform grid solution terminated at the next time step because of negative temperatures caused by the oscilllations.

Therefore, with the same number of grid points an unusable calculation has been converted to an efficient and accurate one. However, some new, but minor, problems have been introduced with this remedy. One of these problems is caused when the thin flame passes out of the boundaries of the system and there are no longer any gradients along some of the fixed arcs. The grid then reverts back to a uniform grid over one time step. In the present calculation, this does not cause a problem because the dependent variable is uniform and the rapid change in metrics is unimportant because the

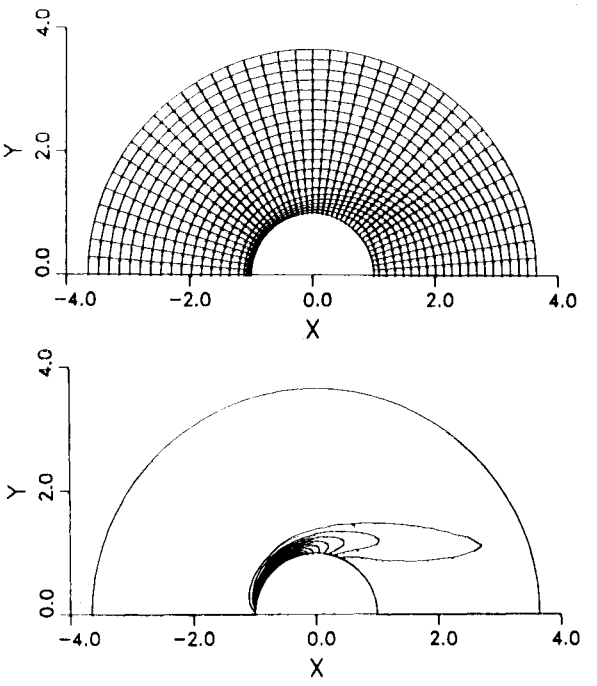

Fig. 13 Vorticity and coordinate distribution for separated flow with $Re = 100$.

solution is not changing. However, if another variable such as velocity was being calculated in this region, it would be extremely difficult to obtain an accurate solution for that variable.

The grid adaption which has occurred in the previous graphs was accomplished by placing grid points along fixed radial lines. It is the opinion of the present authors that fixing one set of coordinate lines can offer an advantage in many physical problems, since full adaption in two dimensions can lead to highly skewed and unusable grid systems. Investigators can also have the advantage of using their knowledge of the physics of the problem to choose this initial and fixed set of grid lines. Frequently, the result is that the problem becomes quasi-one-dimensional, as in the previous calculations, and this surely can be one of the most efficient and accurate ways to numerically calculate thin convective-diffusive regions. However, many problems need full adaption and there is certainly a need for many techniques in adaptive numerical methods.

A Reminder on Variable Grids

It is obvious from the previous results that the grid changes rapidly as one moves into a high gradient zone. The widely held belief for situations with rapidly varying grids is that the numerical simulation is inaccurate; however, it is shown clearly that this is not the situation with an adaptive grid. When the grid and solution are coupled together the solution is accurate and rapid changes in grid reflect the solution taking on constant or slowing varying changes.

Adaptive Gridding in Separated Flows

Until the present time only results with rather simple fluid mechanics have been presented herein. As an example of the use of adaptive gridding with complicated fluid dynamics, the ignition problem presented previously with a Stokes low Reynolds number velocity field will be resolved with an incompressible separated flow over a sphere at a Reynolds number of 100. This problem is particularly troublesome because the fluid dynamics form different regions of small scale at different locations in space. In fact, it is the present author's opinion that the flame zone and boundary layers are incompatible geometries and two separate adaptive grids are

needed for the problem. Therefore, the calculation has been carried out with two separate grid systems, one for fluid mechanics and one for flame propagation.

A result from this calculation is shown in Figs. 12 and 13 where the flame has almost been convected out of the computational zone. Figure 12 shows the entire computational zone for the flame and it is immediately clear that the free, separated shear layer has had a large influence on the flame location. Also, it is clear that the adaptive gridding method ($R_1 = 1/7$, $R_2 = 0$) has not had any difficulty with this entirely different shape compared to the previous problem.

Figure 13 shows the inner part of the grid and vorticity distribution for the separated fluid mechanics, the full grid extends from $-15 \le x \le 15$. Ten normalized vorticity contours, normalized with the maximum surface vorticity, are shown to illustrate the separated nature of the flow, and it is visually obvious that the adaptive grid reflects the structure of the flow. The calculated drag agrees quite well with other investigators[5] who utilized spherically symmetric expanded grids. The major improvement of the adaptive calculation is in the prediction of the size of separated flow bubble and not the prediction of drag. Geometrically expanded grids which are surface oriented accurately resolve the boundary layer, but result in incorrect scaling in the wake. For the same number of grid points the adaptive calculation will properly scale both the boundary layer and separated flow region. Therefore, with a fewer number of grid points, a more accurate calculation is obtained.

The variable used for grid adaption for the fluid mechanics was the velocity gradient $\partial v_\theta / \partial r$, where r is the radial coordinate. This choice was good everywhere except near the stagnation points where considerable trouble is caused by the line of symmetry boundary condition. The problem is easily removed by not adapting in the region $0 \le \theta \le 15$ deg and using the grid distribution obtained at $\theta \simeq 15$ deg for this stagnation region. For this separated flow it is not clear what dependent variable should be used for adaption and at the present time we are working on an improved strategy.

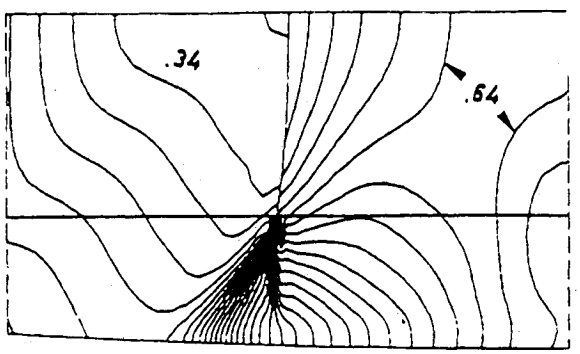

Fig. 14 Isobars from ONERA calculation.[6]

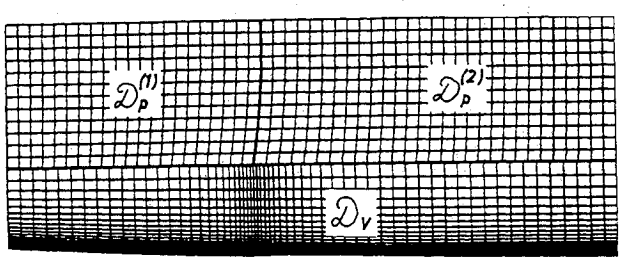

Fig. 15 Coordinate system of ONERA calculation.[6]

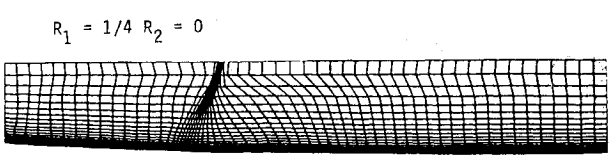

Fig. 16 Adaptive coordinates for ONERA calculation; $R_1 = 1/4$, $R_2 = 0$.

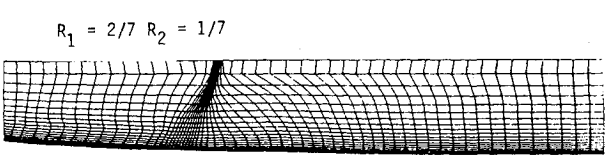

Fig. 17 Adaptive coordinates for ONERA calculation; $R_1 = 2/7$, $R_2 = 1/7$.

Preliminary Results for Shock/Boundary-Layer Interaction

The author has recently returned from a technical visit to the French laboratory ONERA where the adaptive techniques presented here were applied to a calculation carried out by that laboratory. The adaptive method was applied to a shock/boundary-layer interaction calculation previously completed at ONERA,[6] but a new calculation with the adaptive grid was not carried out. In order to show some additional characteristics of the present technique, we have decided to show these results.

The original ONERA calculation consisted of a compressible Navier-Stokes nozzle wall calculation with a rectangular grid, and a geometrically expanded grid about a fitted shock in the inviscid portion of the flow. Figures 14 and 15 show the grid system and calculated isobars respectively, and the viscous region is shown by the symbol $\mathcal{D}_v$. For this problem, it was decided to adapt along the lines semiparallel to the wall, and thus they remained fixed during adaption. The variable chosen for adaption was the pressure field and adaption was carried out with both a first and second derivative dependence. The results of some adaptive calculations are shown in Figs. 16 and 17, where the adaptive grids are shown.

Figure 16 contains only first derivative adaption, $R_1 = 1/4$ and $R_2 = 0$, and the system reflects the isobar patterns very closely in Fig. 15. The results in Fig. 17 utilized both first and second difference adaption, $R_1 = 2/7$ and $R_2 = 1/7$, and are characterized by the anticipation of the high gradient region due to the second difference influence. Although the second difference results yield a somewhat smoother grid, they also cause the grid to become nonperpendicular to the wall. Since the pressure is essentially constant across the boundary layer, this is not a problem for the first derivative strategy by itself. Of course, without redoing the calculation one cannot make any firm judgments on the "goodness" of the grids, but certainly the wall angle of the grid should be watched closely. However, the grid systems generated do seem quite promising and may offer significant advantages for problems of this type.

Summary and Conclusions

The present paper contains the results of the successful application of an adaptive grid technique to a wide variety of problems in fluid mechanics and heat transfer. The highlights of these results are:

1) An a priori assignment of the maximum allowable change in a dependent variable between grid points can be achieved with first derivative adaption.

2) With the present adaptive grid method, one knows in advance the number of grid points utilized in resolving the geometric features of the boundaries, the function change, and the slope change of the function.

3) Highly variable step sizes which result from adaptive gridding do not seem to cause inaccuracies in the evaluation of finite difference expressions. This result was obtained from numerical experimentation and theoretical verification has not been carried out. However, the method strongly couples grid variation with function variation and this result does not seem to be surprising to the present investigator.

4) The problem of cell Reynolds number which is caused by high gradient convective-diffusive regions is removed in principle with first derivative adaption. With all the problems in the present paper, it has also been removed in practice and it seems that this thorny problem will give way to adaptive gridding techniques.

5) With the cell Reynolds problem removed by adaptive techniques, most finite difference techniques will yield good results in high gradient convective-diffusive zones. First-order windward techniques will not cause artificial diffusion and higher-order techniques will not oscillate.

6) Windward difference techniques appear to be good to use when searching for an adaptive grid. Their damping properties on course grids and their strong diagonal dominance properties are highly desirable when one is converging on a grid. The converged solution will not contain artificial diffusion and one should be able to change easily to a higher-order method.

7) For multidimensional problems with embedded high gradient regions of a convective-diffusive nature, first derivative adaption generates a grid which can be characterized as quasi-one-dimensional. On this grid, cross derivatives in space, caused by generalized coordinates, are almost zero in the high gradient zone. This quasi-one-dimensional grid is very efficient for solving the problem and improves the convergence and stability properties of the first- and second-order difference schemes used in the paper.

8) The present method requires the generation and choice of a fixed set of grid lines in multidimensional problems. This requirement can be both a strength and weakness of the technique. It is a strength when the physics of the problems clearly suggests the direction of the body-oriented fixed grid lines. It is a weakness when the given problem does not have a preferred direction and fixed lines are not appropriate. In this situation a full multidimensional technique will be required.[8] However, it is the present author's opinion that a very large portion of the problems with embedded, high gradient, convective-diffusive regions can be treated in a very efficient way with the present methods used in the paper.

Acknowledgments

The authors would like to thank Sandia Laboratories, Livermore, Calif., and ONERA, Chatillon, France, for the considerable help and support that they have given to this research effort. In particular, the author is very grateful for the discussions and encouragement given to him by Dr. R. J. Kee of Sandia and Dr. H. Viviand of ONERA—it is always much easier to carry out research in a stimulating environment.

References

[1] Dwyer, H. A., Kee, R. J., Barr, P. K., and Sanders, B. R., "Transient Droplet Heating at High Peclet Number," Paper presented at ASME Winter Annual Meeting, Symposium on Computers and Fluids, Nov. 1981, to appear in *Journal of Heat Transfer.*

[2] Dwyer, H. A., Kee, R. J., and Sanders, B. R., "Adaptive Grid Method for Problems in Fluid Mechanics and Heat Transfer," *AIAA Journal*, Vol. 18, Oct. 1980, p. 1205.

[3] Dwyer, H. A., Sanders, B. R., and Raiszadeh, F., "Ignition and Flame Propagation Studies with Adaptive Numerical Grids," to appear in *Combustion and Flame.*

[4] Roache, P., *Computational Fluid Dynamics*, Hermosa Publishers, Albuquerque, New Mex., 1971.

[5] Clift, R., Grace, J. R., and Weber, M. E., *Bubbles, Drops and Particles*, Academic Press, New York, 1978.

[6] Cambier, L., Ghanzi, W., Veuillot, J. P., and Viviand, H., "Une Approche Par Domaines Pour Le Calcul D'Ecoulements Compressibles," ONERA TP 1981-143, 1981.

[7] Gelinas, R. J., Doss, S., and Miller, K., "The Moving Method: Applications to General Partial Differential Equations with Multiple Large Gradients," *Journal of Computational Physics*, Vol. 40, March 1981, p. 202.

[8] Brockbill, J. U. and Saltzman, "Adaptive Zoning for a Singular Problem in Two Dimensions," LA-UR-81-405, Los Alamos Scientific Laboratory, Los Alamos, New Mex., 1981.